

See discussions, stats, and author profiles for this publication at: <https://www.researchgate.net/publication/270590659>

# Hydrazine-Free Surface Modification of CZTSe Nanocrystals with All-Inorganic Ligand

ARTICLE *in* THE JOURNAL OF PHYSICAL CHEMISTRY C · DECEMBER 2014

Impact Factor: 4.77 · DOI: 10.1021/jp510558b

---

CITATIONS

3

READS

118

## 11 AUTHORS, INCLUDING:



[Chaochao Dun](#)

Wake Forest University

28 PUBLICATIONS 80 CITATIONS

[SEE PROFILE](#)



[Wanyi Nie](#)

Wake Forest University

28 PUBLICATIONS 322 CITATIONS

[SEE PROFILE](#)



[Yuan Li](#)

Wake Forest University

56 PUBLICATIONS 543 CITATIONS

[SEE PROFILE](#)



[David Carroll](#)

Wake Forest University

264 PUBLICATIONS 10,416 CITATIONS

[SEE PROFILE](#)

# Hydrazine-Free Surface Modification of CZTSe Nanocrystals with All-Inorganic Ligand

Chaochao Dun,<sup>†</sup> Wenxiao Huang,<sup>†</sup> Huihui Huang,<sup>†</sup> Junwei Xu,<sup>†</sup> Ning Zhou,<sup>‡</sup> Ye Zheng,<sup>§</sup> Hsinhan Tsai,<sup>||</sup> Wanyi Nie,<sup>||</sup> Drew R. Onken,<sup>†</sup> Yuan Li,<sup>\*,†</sup> and David L. Carroll<sup>\*,†</sup>

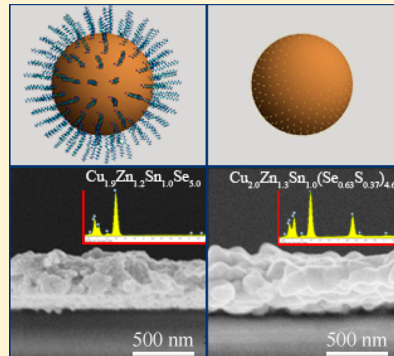
<sup>†</sup>Center for Nanotechnology and Molecular Materials, Department of Physics and <sup>§</sup>Department of Chemistry, Wake Forest University, Winston-Salem, North Carolina 27109, United States

<sup>‡</sup>State Key Laboratory for Diagnosis and Treatment of Infectious Diseases, The First Affiliated Hospital, Zhejiang University School of Medicine, Hangzhou, Zhejiang 310003, P. R. China

<sup>||</sup>Chemistry Division, Los Alamos National Laboratory, Los Alamos, New Mexico 87544, United States

## S Supporting Information

**ABSTRACT:** The optoelectronic properties of semiconductor nanoparticles (NPs) depend sensitively on their surface ligands. However, introducing certain organic ligands to the solution-synthesized CZTSe NPs unfavorably suppresses the interaction among those NPs. These organic ligands prevent the NPs from dissolving in water and create an insulating barrier for charge transportation, which is the key property for semiconductor devices. In our study, by adopting Na<sub>2</sub>S to displace the associated organic ligands on Cu<sub>2</sub>ZnSnSe<sub>4</sub> (CZTSe), we obtained high solubility NPs in an environmentally friendly polar solvent as well as excellent charge transport properties. Toxicity of CZTSe: Na<sub>2</sub>S NPs was determined to be around 10 mg/L. Because of the inorganic ligand S<sup>2-</sup> around CZTSe NPs, thin films can be easily fabricated by solution processing out of benign solvents like water and ethanol. After annealing, a homogeneous CZTSSe absorbing layer without carbon point defects was obtained. As the S<sup>2-</sup> effectively facilitates the electronic coupling in nanocrystal thin films, carrier mobility of the surface-engineered CZTSe enhances from 4.8 to 8.9 cm<sup>2</sup>/(Vs). This raises the possibility for engineering chalcogenide materials by controlling the surface properties during the fabrication process.



## I. INTRODUCTION

Inorganic nanoparticles (NPs) such as CdSe/CdTe,<sup>1</sup> Cu<sub>2</sub>ZnSnSe<sub>4</sub> (CZTSe),<sup>2</sup> and metal oxides<sup>3</sup> are believed to possess promising potential as high efficiency photovoltaics (PVs),<sup>1,4</sup> thermal-electrical materials,<sup>2</sup> and light-emitting diodes.<sup>3</sup> Although each type of nanocrystal holds its own size-dependent properties, the charge carrier transportation is dominated by the interparticle medium.<sup>5-7</sup> It is therefore fundamentally important to engineer the surface properties of NPs to achieve high transport properties as well as ease of processing. As is well-known, the essential function of the coordinating solvents (ligand, surfactant, etc.) in the solution-based methods is to prevent aggregation and increase stability of the inorganic NPs.<sup>8</sup> However, as these organic additives unfavorably suppress the interaction of neighboring NPs by introducing an insulating barrier, larger amounts of ligands bounded to the NPs surface are detrimental to the electronic coupling between adjacent NPs. Moreover, once the NPs are made into thin films, the ligands introduce a density of undesirable surface defects (such as cracking and voids) that can become significant traps to lower the semiconductor device performance, especially after annealing at high temperature. Considerable efforts have been made to overcome such problems. For example, the surface modification approach

uses smaller capping molecules, including both organic short alkyl chain molecules<sup>9-12</sup> and inorganic capping agents.<sup>5-7,13</sup> These methods have achieved varying degrees of success in terms of attaining a highly disperse state and acquiring enhanced electronic communication. However, the involved hydrazine is explosive, pyrophoric, and carcinogenic, which becomes the major drawback when it comes to broad applications. At the same time, using the less toxic inorganic S<sup>2-</sup><sup>14</sup> as a surface ligand attached to the NPs is found to provide the electrostatic stabilization for NPs to disperse them in variety of polar solvents. For example, the traditional CdSe quantum dots (QDs) capped with organic oleic acid and oleylamine could be transferred to a polar solvent without affecting their quantum effect after ligand exchange using (NH<sub>4</sub>)<sub>2</sub>S as a surface ligand.<sup>14,15</sup>

Chalcogenide PVs based on Cu<sub>2</sub>ZnSnS<sub>4</sub> (CZTS) and CZTSe, one of the most promising NPs that can be used as an absorbing layer in high-efficiency thin film solar cells,<sup>4,16-19</sup> have achieved power conversion efficiencies (PCE) as high as 12.6%.<sup>4</sup> One commonly utilized method to fabricate CZTS/

Received: October 20, 2014

Revised: November 29, 2014

CZTSe devices involves the colloidal nanoparticle ink, followed by nonvacuum deposition.<sup>17,20,21</sup> However, the above-mentioned issue will again become a big concern for depositing those NPs into a thin film for a solar cell. Specially, the CZTS/CZTSe NPs adopted large organic surface ligands like oleylamine (OLA), oleic acid, or octylphosphine oxide (TOPO) as capping/stabilizing reaction solvents. Those ligands lead to poor transport properties due to the insulating nature and possible defects after high temperature sintering that could kill the device performance. Moreover, those organic ligands would only allow the NPs to dissolve in hexane and toluene solvents, which are highly toxic. Thus, further improvements in charge transport, conductivity, and decreasing toxicity in the CZTS/Se absorbing thin film are urgently needed and will require new ligands to be developed for this material system.

It has been reported that sodium could significantly improve the PCE of CZTS/CZTSe solar cell device<sup>22,23</sup> by increasing the carrier density and elongating the carrier lifetime. In this paper, by taking advantage of sodium as well as reducing the amount of long hydrocarbon molecules at the surface of the NPs, we used Na<sub>2</sub>S to implement the chemical modification of CZTSe NPs. It is worth mentioning that Na<sub>2</sub>S serves several purposes: (I) imparting the water solubility by adhering S<sup>2-</sup> to the NC surface and providing colloidal stabilization without introducing foreign toxic metal ions, (II) acting as a functional ligand since it produces sulfur anion which is believed to generate CZTSSe after annealing, (III) providing electronic communication between the NPs, and enhancing the carrier mobility, and (IV) increasing the charge carrier concentration and minority lifetime by incorporating the proper amount of Na<sup>+</sup>. Hydrophilic CZTS/CZTSe NPs fully dissolvable in water/ethanol/formamide were obtained. The toxicity of these NPs was determined to be around 10 mg/L. Because of the presence of sulfur without carbon, considerable enhancement of carrier mobility  $\mu$  up to  $8.9 \text{ cm}^2 \text{ V}^{-1} \text{ s}^{-1}$  was achieved. As the commercial photovoltaic relies strongly on high carrier mobility and efficient transport of charge carrier, it is therefore reasonable to predict that CZTSSe-based PV devices might be fabricated by using the present engineered all-inorganic CZTSe. Also, these surface-charged NPs could be utilized for electrostatically driven self-assembly when combining two oppositely charged species.

## II. EXPERIMENTAL METHODS

**A. General Information.** Copper(II) acetylacetone (98+%), zinc acetylacetone (98%), tin(IV) bis (acetylacetone) dichloride (98%), selenium powder (99.7%), oleylamine (OLA, 70%), trioctylphosphine oxide (TOPO, 99%), sodium borohydride (NaBH<sub>4</sub>, 98%), and sodium sulfide nonahydrate (Na<sub>2</sub>S, 98%) were used as received.

**B. Synthesis of CZTSe NPs.** CZTSe NPs were synthesized by hot injection method according to literature.<sup>24</sup> Briefly, Se power is reduced by NaBH<sub>4</sub> with the assistance of ultrasonication in the presence of OLA. OLA is believed to control the growth and stability of CZTSe NPs. The reacting metal compounds were mixed with selenium in OLA and TOPO.

**C. Ligand Exchange of CZTSe NPs.** Ten milliliters (~30 mg/mL) CZTSe NPs dispersed in hexane was combined with 0.55 g Na<sub>2</sub>S that is fully dispersed in 45 mL formamide. The ligand exchange process was performed by vigorously stirring the resulting mixture overnight. All the heterogeneous reactions were carried out under ambient condition. After ligand exchange, the solution was allowed to separate into organic

(upper) and inorganic (bottom) layers, as shown in Figure 1. The surface-modified NPs were then precipitated by adding 10

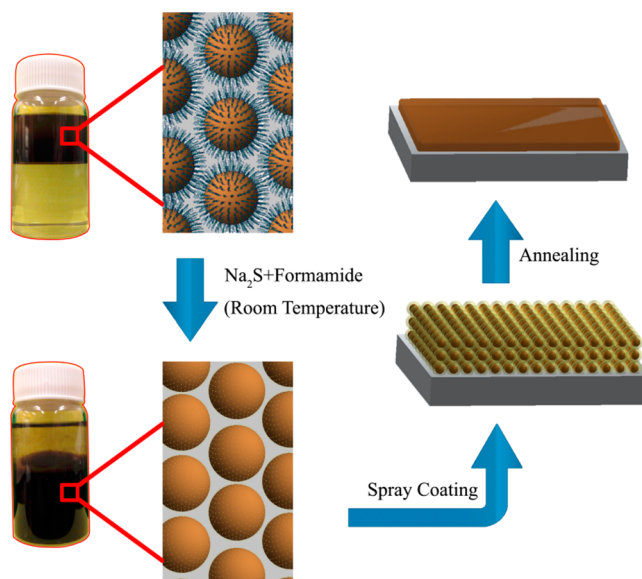


**Figure 1.** Schematic illustration of the ligand exchange process to produce all inorganic nanoparticles and subsequent sprayed CZTSe thin film. The chemical modification process is performed under room temperature.

mL isopropanol and centrifuged to remove the supernatant that contains hexane. To purify the NPs and remove the excessive Na<sup>+</sup>, 2 mL deionized water was added to redisperse the NPs. The aqueous media was subsequently sonicated for 3 min. After that, isopropanol was added again and the mixture was centrifuged at 5000 rpm for 5 min. The supernatant liquid (both deionized water and isopropanol) was then removed. This purification process was repeated at least three times to remove any trace of insoluble materials. Finally, the precipitated CZTSe NPs were dissolved in ethanol for spray coating.

## D. Cytotoxicity of CZTSe:Na<sub>2</sub>S NPs Measurement.

Refer to Supporting Information.

## III. RESULTS AND DISCUSSION

**A. CZTSe NPs Characterization.** The ligand exchange process of OLA displacement with Na<sub>2</sub>S is illustrated in Figure 1. Compared with the long length of OLA-capped NPs, the S<sup>2-</sup>-capped NPs are considered to be nearly “naked”. Moreover, in comparison to the NPs capped with short alkyl chain molecules,<sup>9–11</sup> the present S<sup>2-</sup>-capped NPs are less sensitive to oxidation and thermal degradation. After ligand exchange, the surface of CZTSe NPs is negatively charged, which encourages the stable dispersion of NPs in polar solvent by introducing the electrostatic repulsion. It is shown that the nanocrystal dispersion ability is closely related with the solvent dielectric constant  $\epsilon$ .<sup>25</sup> The higher the value of  $\epsilon$  is, the better the solubility of the NPs when the surfaces of NPs are negatively (or positively) charged. The hydrophilic S<sup>2-</sup>-capped CZTSe NPs we synthesized are fully dissolvable in various polar solvents, including formamide ( $\epsilon = 111$ ), water ( $\epsilon = 80.1$ ), and ethanol ( $\epsilon = 24.5$ ), which are stable for at least 1–2 weeks in the air. This enables thin film formation by solution processing, such as spray coating, in a wide variety of solvents. At the same time, all S<sup>2-</sup>-attached CZTSe NPs lost solubility in nonpolar solvents. Upon thermal annealing, the deposited all-

inorganic NPs could form a crack-free thin film since there is less/no volume reduction associated with organics decomposition. Because of the presence of sulfur, a CZTSSe thin film is believed to form after annealing. Thus, the implementation of bifunctional  $S^{2-}$  ligand is expected to yield enhanced chemical and optoelectronic properties in the resulting CZTSe NPs.

**A.1. Characteristics of the Fabricated NPs.** These all-inorganic CZTSe nanoparticles are dissolvable in hydrophilic solvents. The crystal structures and morphologies of the CZTSe NPs before and after ligand exchange are characterized by using TEM, as shown in Figure 2. Before ligand exchange, all

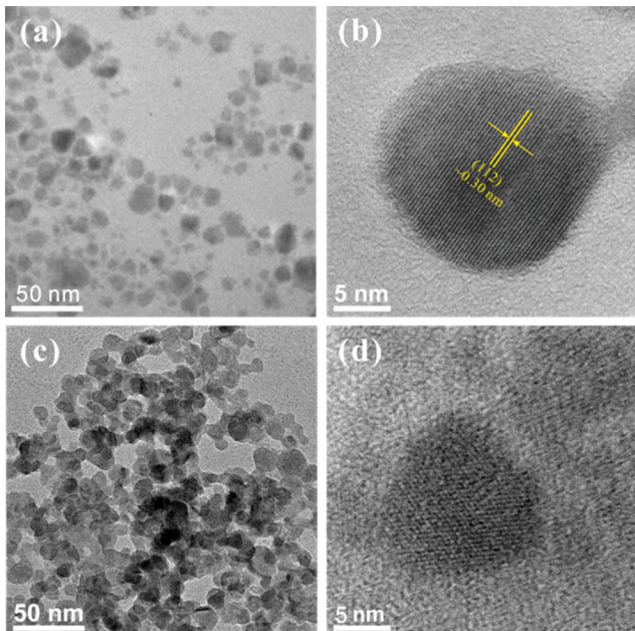
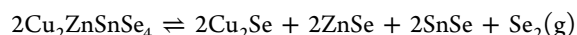


Figure 2. TEM and HRTEM photographs of colloidal solutions. TEM images of CZTSe: (a) capped with original organic ligands OLA in hexane; (c) capped with inorganic ligands  $S^{2-}$  in water. (b,d) Corresponding HRTEM showing the crystal structure in each NP, respectively.

the NPs show pebble-like shapes, with the average particle size around 20 nm. Also, a high resolution TEM (HRTEM) image

of the regular lattice fringes indicates that the NPs are highly crystalline, with characteristic interplanar distance of  $\sim 0.3$  nm from (112) plane of kesterite CZTSe phase. After ligand exchange, there are no apparent crystal structure or shape variations. While the size distribution remains almost unchanged, it is shown that the interparticle distance is reduced to the extent that even slight agglomeration happens. It is expected that the decrease of the interparticle distance can eliminate the influence of the insulating barrier, which might promote the electronic coupling in nanocrystal solids.

**A.2. Ligand Exchange Characterization.** The efficacy of ligand exchange was further studied by Fourier transform infrared spectroscopy (FTIR) and thermogravimetric analysis (TGA). Figure 3a shows the FTIR spectra of dried CZTSe:OLA and CZTSe: $Na_2S$  NPs. The intensity of the characteristic C—H stretch at  $2800\text{--}3000\text{ cm}^{-1}$  that is ascribed to OLA is dramatically reduced after chemical modification, demonstrating that the ligand exchange strategy using  $Na_2S$  effectively eliminates carbon from the NPs. The completeness of the ligand exchange was similar to those using metal chalcogenide complexes (MCC),<sup>26</sup> but without any toxic solutions. TGA is also performed, as shown in Figure 3b, which indicates weight loss as low as 15% compared with the high value of 30% before ligand exchange. The higher mass loss of CZTSe:OLA NPs is caused by the decomposition of bulk OLA molecules. Therefore, it is predictable that the concentrated CZTSe: $Na_2S$  solutions have the ability to remove the organic ligand. It is noteworthy that even the engineered all-inorganic CZTSe loses 15% of its original mass. One of the reasons is the partial decomposition of CZTSe (or CZTSSe) under the annealing process, which is



Without supplying the additional Se vapor pressure, CZTSe powder will decompose, leading to the loss of small amounts of vapor products.<sup>27</sup>

XPS analysis is used to study the valence state of all elements in the as-synthesized hydrophilic CZTSe NPs, as shown in Supporting Information Figure 1S. According to the peak splitting, valence states of Cu, Zn, Sn, and Se are determined as  $Cu^{+}$ ,  $Zn^{2+}$ ,  $Sn^{4+}$ , and  $Se^{2-}$ , as expected. At the same time, the inorganic ligand S is found to be in the  $S^{2-}$  state.<sup>28</sup> The average

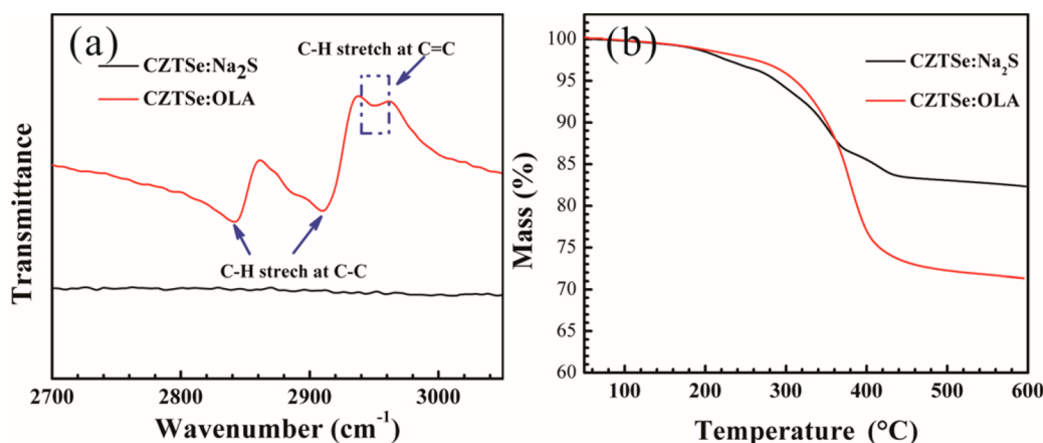
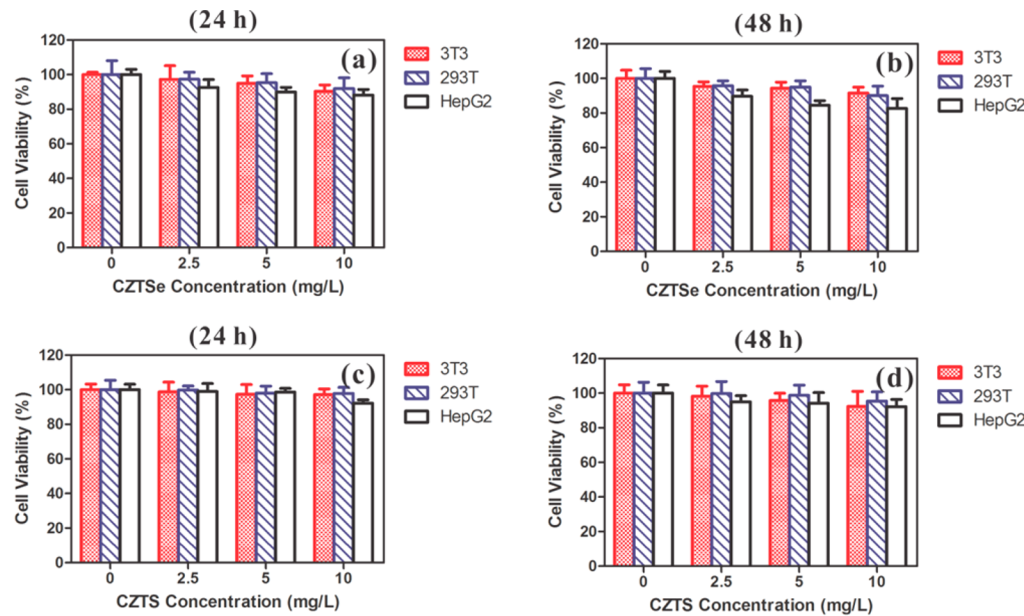


Figure 3. FTIR and TGA for CZTSe NPs capped with long chain organic ligands OLA (red line) and with short inorganic ligands  $Na_2S$  (black line). (a) FTIR illustrates the absence of  $C=C—H$  stretch and C—H stretch absorption in the surface-modified CZTSe after ligand exchange. The FTIR spectra were normalized to the amount of absorbing materials and curves were offset vertically for clarity. (b) TGA indicates weight loss as low as 15% after ligand exchange.



**Figure 4.** Cytotoxicity of CZTSe (a,b) and CZTS (c,d) nanoparticles (dissolved in water) examined by the MTT assay. Cells treated with 0, 2.5, 5, and 10 mg/L concentrations of CZTSe for 24 and 48 h, respectively.

composition of the nanocrystals was determined by EDS (Supporting Information Figure 2S). We take tin as the basis such that the composition takes the form  $\text{Cu}_x\text{Zn}_y\text{Sn}_{1.0}\text{Se}_z$ . Considering the  $\pm 2\%$  uncertainty, the average elemental composition data was  $\text{Cu}_{1.9}\text{Zn}_{1.2}\text{Sn}_{1.0}\text{Se}_{5.0}$  before ligand exchange. After being surface engineered, however, the elemental composition data changes into  $\text{Cu}_{2.0}\text{Zn}_{1.3}\text{Sn}_{1.0}(\text{Se}_{0.63}\text{S}_{0.37})_{4.6}$ . The annealing treatment with glass cover did not alter the compositional notably, which is consistent with the previous literature.<sup>29</sup> It was demonstrated by Scragg et al. that the stability of CZTS/CZTSe can be achieved by either providing the S/Se vapor or putting on a glass cover, with the latter offering a relatively closed system and a chemical equilibrium above the CZTS/CZTSe surface to prevent the decomposition. In our case, the surface ligand  $\text{S}^{2-}$  could provide a sulfur-rich microenvironment as the S vapor does. The elements ratio with  $\text{Cu}/(\text{Zn} + \text{Sn}) = 0.86 - 0.87$ , and  $\text{Zn/Sn} = 1.2 - 1.3$  that deviated from the stoichiometry, is exactly in the range that could yield the highest solar cell efficiency.<sup>20,30</sup> Also, the ratio of  $\text{Se}/(\text{S} + \text{Se})$  is determined to be 0.67 here. As is known, the grain size of pure CZTS is smaller than CZTSe, which means CZTSe has less grain boundary scattering. At the same time, because the atomic scattering factor for Se is higher than that of S, the CZTSe has a higher atomic scattering ability. Se-rich CZTSSe compounds are verified to optimize these two factors,<sup>4,31</sup> which can also be obtained by the present surface engineering process.

**A.3. Cytotoxicity of CZTSe Nanoparticles.** The toxicity of NPs is a natural concern because of their potential for applications in solar cells. Here, the cytotoxicity of CZTSe nanoparticles was examined by the MTT assay (for details, see Supporting Information). By using various cells, cytotoxicity of ligand exchanged CZTSe:Na<sub>2</sub>S is evaluated to possess low toxicity around 10 mg/L (Figure 4 and Supporting Information Figure 3S). In order to compare different cell viability in the presence of CZTSe:Na<sub>2</sub>S nanoparticles, we have tested three different kinds of human cells: 3T3, 293T, and HepG<sub>2</sub> cells. Cells treated with 2.5, 5, and 10 mg/L concentrations of

CZTSe for 24 and 48 h were subjected to the MTT assay for cell-viability determination, respectively. Control experiments were conducted in a similar manner without the presence of CZTSe nanoparticles.

As shown in Figure 4a,b, after 48 h of CZTSe treatment, 3T3 and 293T cells with concentrations up to 10 mg/L still show more than 90% viability. Cell viability data indicated that the CZTSe nanoparticles did not significantly affect cell proliferation. Therefore, the results suggest that the CZTSe nanoparticles have reasonably little toxicity and are biocompatible up to the given concentrations. The cytotoxicity of CZTS:Na<sub>2</sub>S nanoparticles was examined using the same method. After 48 h of CZTS treatment, all 3T3, 293T, and HepG<sub>2</sub> cells showed more than 90% viability at 10 mg/L concentrations (Figure 4c,d), demonstrating that the CZTS nanoparticles were also biocompatible at the given concentrations.

To further study the effect of CZTSe:Na<sub>2</sub>S nanoparticles on cell morphologies, we labeled 3T3, 293T, and HepG<sub>2</sub> cells with FDA (Fluorescein Diacetate) under a fluorescent microscope. Supporting Information Figure 3S shows the typical fluorescence microscopy images of untreated control 293T cells and the cells treated with different concentrations of CZTSe nanoparticles for 48 h. In FDA-stained cells, the live cell fluorescence was bright green. It was shown here that there was no obvious change of cell morphologies after exposure to the CZTSe nanoparticles for 2 days even at the highest concentration 10 mg/L. Previously, it was reported by Wu et al.<sup>32</sup> that MoS<sub>2</sub> nanoparticles have little cytotoxicity after exposure to low concentration (3.52 mg/L). Besides, Grabinski et al.<sup>33</sup> reported that the cell viability started to decrease after exposure to 5 mg/L of MWCNT (multiwalled carbon nanotubes) and SWCNT (single-walled carbon nanotubes) for 24 h. Comparing cytotoxicity of CZTSe with MoS<sub>2</sub> nanoparticles and carbon nanomaterials, CZTSe nanoparticles have a comparable biocompatibility (10 mg/L) with the vitro cells.

**B. Thin Films of CZTSe:OLA and CZTSe:Na<sub>2</sub>S.** *B.1. Thin Film Morphology.* The thin film morphology is studied before and after S<sup>2-</sup> modification by SEM in Figure 5. Thin films of

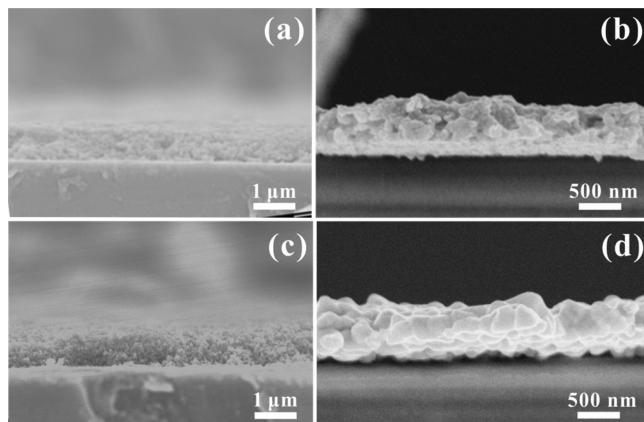


**Figure 5.** Cross-sectional SEM of CZTSe:OLA and CZTSe:Na<sub>2</sub>S thin films before and after annealing (under 350 °C): (a) CZTSe:OLA before annealing; (b) CZTSe:OLA after low temperature annealing; (c) CZTSe:Na<sub>2</sub>S before annealing; (d) CZTSe:Na<sub>2</sub>S after low temperature annealing.

S<sup>2-</sup>-capped CZTSe nanocrystals were prepared by spray-coating nanocrystal solutions (ethanol) onto glass with ITO and then annealing at a relatively low temperature 350 °C for 30 min. To prevent a side reaction that relates to metal oxides,<sup>34</sup> care was taken to ensure that no oxygen remained in the annealing process. Also, in order to prevent the decomposition of CZTSe as suggested by the TGA data, thin film of CZTSe capped with S<sup>2-</sup> was placed under a small glass cover.<sup>29</sup> As there is no additional decomposition or related volume contraction for the engineered CZTSe, the fabricated dense semiconductor thin film could prevent defects like cracking and voids in the annealing process, as can be seen from Figure 5. In comparison with Figure 5b and d, although both cases show certain growth of the grain size, it is confirmed that the NPs become much more compacted without voids in the vertical directions for the engineered CZTSe thin film. The disappearance of the insulating organic ligands and subsequent carbon point defects would create a more conductive film.

**B.2. Thin Film Crystal Formation.** To confirm the crystal structure for the synthesized nanocrystals, we ran X-ray diffraction and Raman spectroscopy on the respective thin film. Figure 6a shows the XRD diffraction patterns of the as-fabricated and surface-engineered NP-based thin films before annealing, which correspond to CZTSe (JCPDS No.70–8930).

To gain further insight into the potential impurities like ZnS and Cu<sub>2</sub>SnS<sub>3</sub>, Raman spectra of the deposited CZTSe thin film before and after ligand exchange were obtained, as shown in Figure 6b. Both patterns show Raman peaks at 81, 174, 196, and 235 cm<sup>-1</sup> that are attributed to E (TO LO) symmetry modes, two minor A modes, the main A mode, and B (TO LO) symmetry modes, respectively. This is in great agreement with previous experimental<sup>13</sup> and simulated<sup>35,36</sup> results. Therefore, either XRD or Raman measurement shows undetectable secondary phases. Also, XRD and Raman results do not reveal noticeable crystal changes, confirming that the ligand exchange did not change the structure of CZTSe NPs.

Figure 7a shows the XRD patterns for the annealed CZTSe:OLA and CZTSe:Na<sub>2</sub>S deposited thin film. After annealing, diffraction peaks become sharper compared with XRD patterns before thermal treatment, suggesting the formation of crystalline quaternary semiconductors. The sharp peaks of the CZTSe:OLA thin films are confirmed to be  $2\theta = 27.3^\circ$ ,  $45.2^\circ$ , and  $53.4^\circ$ , which correspond to the diffraction planes (112), (204)/(220), and (312), respectively. On the other hand, Figure 7b,c illustrates the enlargement of  $2\theta$  angles around the respective peaks. After annealing, the diffraction peaks of CZTSe:Na<sub>2</sub>S shift to higher values of  $2\theta$ , corresponding to smaller lattice spacing. Because of the integration of attached S atoms into the original CZTSe, the lattice parameters decrease as expected. This result suggests that binding negatively charged S<sup>2-</sup> ions are attached to CZTSe NC surface. After annealing, a reaction between S<sup>2-</sup> and CZTSe NPs is triggered, which leads to the formation of CZTSSe.

**B.3. Thin Film Charge Transport Characterization.** Chemical modification of the NP surface is significantly important to the development of solar materials since the surface ligand has a strong relationship with the electrical communication. In order to get at least relative information about the electrical properties, the hole-only device with structure Glass/ITO/CZTSe/MoO<sub>3</sub>/Al was fabricated. It was known that the carrier mobility can be exacted from the J–V characteristics through approximation of the space charge limited current (SCLC)<sup>37</sup> by

$$J = \frac{9}{8} \epsilon_0 \epsilon \mu_0 \exp\left(0.89\beta \sqrt{\frac{V}{d}}\right) \frac{V^2}{d^3}$$

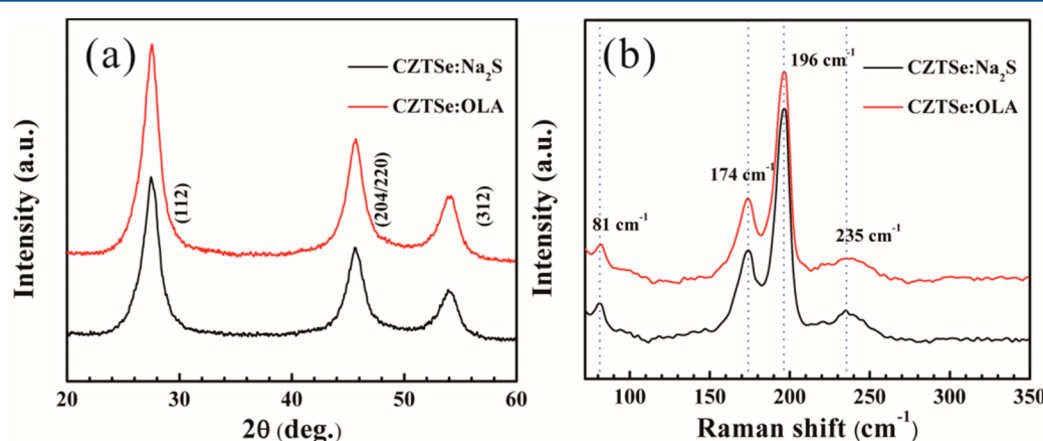


**Figure 6.** XRD and Raman of the sprayed CZTSe:OLA and CZTSe:Na<sub>2</sub>S thin films before annealing.

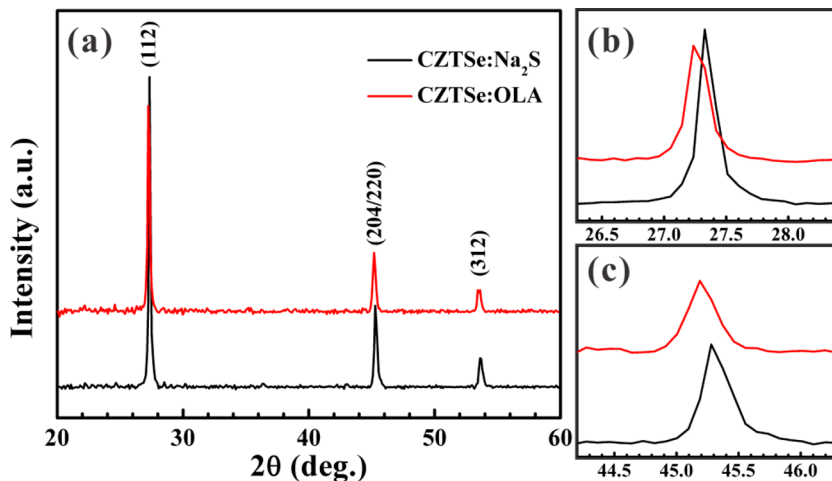


**Figure 7.** XRD of CZTSe:OLA and CZTSe:Na<sub>2</sub>S thin films after annealing.

where  $\mu_0$  is the carrier mobility,  $V$  the applied voltage,  $d$  the thickness of the film,  $\epsilon_0$  the permittivity of free space, and  $\epsilon$  the dielectric constant of CZTSe ( $\epsilon = 8.6^{38}$ ), which determines  $\beta$  by

$$\beta = \frac{1}{k_B T} \left( \frac{q^3}{\pi \epsilon_0 \epsilon} \right)^{1/2}$$

where  $k_B$  denotes the Boltzmann constant,  $T$  the temperature, and  $q$  the elementary charge. Since the deposited post-ligand-exchanged NPs produce a crack-free thin film after annealing, a striking improvement of carrier mobility in CZTSe:Na<sub>2</sub>S is achieved, up to 8.9 from 4.8 cm<sup>2</sup>/(V s) for CZTSe:OLA, suggesting a better carrier transport property to move across from the absorber layer to the electrode without recombination.

#### IV. CONCLUSION

A facile and versatile ligand exchange strategy to modify the surface properties of CZTSe NPs by using the nontoxic solvent Na<sub>2</sub>S is demonstrated. This approach benefits from the combination that Na<sub>2</sub>S not only can remove the long ligand, but also can change the NPs chemical composition to obtain the desired CZTSSe NPs. A nearly carbon-free surface of CZTSe NPs that can be fully dissolved in hydrophilic media is obtained. It is discovered that Na<sub>2</sub>S (I) has the ability to provide colloidal stabilization of the CZTSe NPs by adhering S<sup>2-</sup> to the surface, (II) can facilitate electronic communication between the NPs and enhance the mobility of CZTSe thin film, and (III) enables NPs to be sintered at relatively low temperature while retaining the efficient interparticle transport. This developed approach can potentially improve the performance of CZTSe-based photovoltaics.

#### ■ ASSOCIATED CONTENT

##### Supporting Information

CZTSe NPs synthesis details, toxicity of CZTSe:Na<sub>2</sub>S NPs measurement, thin film fabricating, characterizations including XPS analysis and EDS, and typical fluorescent microscopy images of 293T cells treated with different concentrations of CZTSe nanoparticles. This material is available free of charge via the Internet at <http://pubs.acs.org>.

#### ■ AUTHOR INFORMATION

##### Corresponding Authors

\*E-mail: carroldl@wfu.edu. Phone (office): 336 758 5508. Phone (center): 336 727 1806.

\*E-mail: liy@wfu.edu. Phone (office): 336 758 5508. Phone (center): 336 727 1806.

##### Notes

The authors declare no competing financial interest.

#### ■ ACKNOWLEDGMENTS

The authors would like to acknowledge Dr./Professor Natalie A. W. Holzwarth for fruitful discussions.

#### ■ REFERENCES

- Gur, I.; Fromer, N. A.; Geier, M. L.; Alivisatos, A. P. Air-Stable All-Inorganic Nanocrystal Solar Cells Processed from Solution. *Science* **2005**, *310*, 462–465.
- Fan, F.-J.; Wang, Y.-X.; Liu, X.-J.; Wu, L.; Yu, S.-H. Large-Scale Colloidal Synthesis of Non-Stoichiometric Cu(2) ZnSnSe(4) Nanocrystals for Thermoelectric Applications. *Adv. Mater.* **2012**, *24*, 6158–6163.
- Caruge, J. M.; Halpert, J. E.; Wood, V.; Bulović, V.; Bawendi, M. G. Colloidal Quantum-Dot Light-Emitting Diodes with Metal-Oxide Charge Transport Layers. *Nat. Photonics* **2008**, *2*, 247–250.
- Wang, W.; Winkler, M. T.; Gunawan, O.; Gokmen, T.; Todorov, T. K.; Zhu, Y.; Mitzi, D. B. Device Characteristics of CZTSSe Thin-Film Solar Cells with 12.6% Efficiency. *Adv. Energy Mater.* **2014**, *4*, 1301465.
- Kovalenko, M. V.; Scheele, M.; Talapin, D. V. Colloidal Nanocrystals with Molecular Metal Chalcogenide Surface Ligands. *Science* **2009**, *324*, 1417–1420.
- Lee, J.-S.; Kovalenko, M. V.; Huang, J.; Chung, D. S.; Talapin, D. V. Band-like Transport, High Electron Mobility and High Photoconductivity in All-Inorganic Nanocrystal Arrays. *Nat. Nanotechnol.* **2011**, *6*, 348–352.
- Dong, A.; Ye, X.; Chen, J.; Kang, Y.; Gordon, T.; Kikkawa, J. M.; Murray, C. B. A Generalized Ligand-Exchange Strategy Enabling Sequential Surface Functionalization of Colloidal Nanocrystals. *J. Am. Chem. Soc.* **2011**, *133*, 998–1006.
- Yin, Y.; Alivisatos, A. P. Colloidal Nanocrystal Synthesis and the Organic-Inorganic Interface. *Nature* **2005**, *437*, 664–670.
- Jarosz, M.; Porter, V.; Fisher, B.; Kastner, M.; Bawendi, M. Photoconductivity Studies of Treated CdSe Quantum Dot Films Exhibiting Increased Exciton Ionization Efficiency. *Phys. Rev. B* **2004**, *70*, 195327.

- (10) Luther, J. M.; Law, M.; Song, Q.; Perkins, C. L.; Beard, M. C.; Nozik, A. J. Structural, Optical, and Electrical Properties of Self-Assembled Films of PbSe Nanocrystals Treated with 1,2-Ethanedithiol. *ACS Nano* **2008**, *2*, 271–280.
- (11) Riha, S. C.; Fredrick, S. J.; Sambur, J. B.; Liu, Y.; Prieto, A. L.; Parkinson, B. a. Photoelectrochemical Characterization of Nanocrystalline Thin-Film  $\text{Cu}_2\text{ZnSnS}_4$  Photocathodes. *ACS Appl. Mater. Interfaces* **2011**, *3*, 58–66.
- (12) Huang, W.; Li, Q.; Chen, Y.; Xia, Y.; Huang, H.; Dun, C.; Li, Y.; Carroll, D. L. Surface Modification Enabled Carrier Mobility Adjustment in CZTS Nanoparticle Thin Films. *Sol. Energy Mater. Sol. Cells* **2014**, *127*, 188–192.
- (13) Carrete, A.; Shavel, A.; Fontané, X.; Montserrat, J.; Fan, J.; Ibáñez, M.; Saucedo, E.; Pérez-Rodríguez, A.; Cabot, A. Antimony-Based Ligand Exchange To Promote Crystallization in Spray-Deposited  $\text{Cu}_2\text{ZnSnSe}_4$  Solar Cells. *J. Am. Chem. Soc.* **2013**, *135*, 15982–15985.
- (14) Zhang, H.; Hu, B.; Sun, L.; Hovden, R.; Wise, F. W.; Muller, D. a; Robinson, R. D. Surfactant Ligand Removal and Rational Fabrication of Inorganically Connected Quantum Dots. *Nano Lett.* **2011**, *11*, 5356–5361.
- (15) Choi, S.; Jin, H.; Kim, S.  $\text{SnS}_4^{4-}$  Metal Chalcogenide Ligand,  $\text{S}^{2-}$ -Metal Free Ligand, and Organic Surface Ligand Toward Efficient CdSe Quantum Dot-Sensitized Solar Cells. *J. Phys. Chem. C* **2014**, *118*, 17019.
- (16) Cao, Y.; Denny, M. S.; Caspar, J. V.; Farneth, W. E.; Guo, Q.; Ionkin, A. S.; Johnson, L. K.; Lu, M.; Malajovich, I.; Radu, D.; et al. High-Efficiency Solution-Processed  $\text{Cu}_2\text{ZnSn}(\text{S},\text{Se})_4$  Thin-Film Solar Cells Prepared from Binary and Ternary Nanoparticles. *J. Am. Chem. Soc.* **2012**, *134*, 15644–15647.
- (17) Guo, Q.; Hillhouse, H.; Agrawal, R. Synthesis of  $\text{Cu}_2\text{ZnSnS}_4$  Nanocrystal Ink and Its Use for Solar Cells. *J. Am. Chem. Soc.* **2009**, *131*, 11672–11673.
- (18) Ki, W.; Hillhouse, H. W. Earth-Abundant Element Photovoltaics Directly from Soluble Precursors with High Yield Using a Non-Toxic Solvent. *Adv. Energy Mater.* **2011**, *1*, 732–735.
- (19) Shavel, A.; Cadavid, D.; Ibáñez, M.; Carrete, A.; Cabot, A. Continuous Production of  $\text{Cu}_2\text{ZnSnS}_4$  Nanocrystals in a Flow Reactor. *J. Am. Chem. Soc.* **2012**, *134*, 1438–1441.
- (20) Guo, Q.; Ford, G. M.; Yang, W.-C.; Walker, B. C.; Stach, E. a; Hillhouse, H. W.; Agrawal, R. Fabrication of 7.2% Efficient CZTSSe Solar Cells Using CZTS Nanocrystals. *J. Am. Chem. Soc.* **2010**, *132*, 17384–17386.
- (21) Miskin, C. K.; Yang, W.; Hages, C. J.; Carter, N. J.; Joglekar, C. S.; Stach, E. A.; Agrawal, R. 9.0% Efficient  $\text{Cu}_2\text{ZnSn}(\text{S},\text{Se})_4$  Solar Cells from Selenized Nanoparticle Inks. *Progress in Photovoltaics: Research and Applications* **2014**, *57*, 0–5.
- (22) Li, J. V.; Kuciauskas, D.; Young, M. R.; Repins, I. L. Effects of Sodium Incorporation in Co-Evaporated  $\text{Cu}_2\text{ZnSnSe}_4$  Thin-Film Solar Cells. *Appl. Phys. Lett.* **2013**, *102*, 163905.
- (23) Zhou, H.; Song, T.-B.; Hsu, W.-C.; Luo, S.; Ye, S.; Duan, H.-S.; Hsu, C.-J.; Yang, W.; Yang, Y. Rational Defect Passivation of  $\text{Cu}_2\text{ZnSn}(\text{S},\text{Se})_4$  Photovoltaics with Solution-Processed  $\text{Cu}_2\text{ZnSnS}_4:\text{Na}$  Nanocrystals. *J. Am. Chem. Soc.* **2013**, *135*, 15998–16001.
- (24) Riha, S. C.; Parkinson, B. a; Prieto, A. L. Compositionally Tunable  $\text{Cu}_2\text{ZnSn}(\text{S}_{1-x}\text{Se}_x)_4$  Nanocrystals: Probing the Effect of Se-Inclusion in Mixed Chalcogenide Thin Films. *J. Am. Chem. Soc.* **2011**, *133*, 15272–15275.
- (25) Nag, A.; Kovalenko, M. V.; Lee, J.; Liu, W.; Spokoyny, B.; Talapin, D. V. Metal-free Inorganic Ligands for Colloidal Nanocrystals:  $\text{S}^{2-}$ ,  $\text{HS}^-$ ,  $\text{Se}^{2-}$ ,  $\text{HSe}^-$ ,  $\text{Te}^{2-}$ ,  $\text{HTe}^-$ ,  $\text{TeS}_3^{2-}$ ,  $\text{OH}^-$ , and  $\text{NH}_2^-$  as Surface Ligands. *J. Am. Chem. Soc.* **2011**, *133*, 10612–10620.
- (26) Kovalenko, M. V.; Bodnarchuk, M. I.; Zaumseil, J.; Lee, J.-S.; Talapin, D. V. Expanding the Chemical Versatility of Colloidal Nanocrystals Capped with Molecular Metal Chalcogenide Ligands. *J. Am. Chem. Soc.* **2010**, *132*, 10085–10092.
- (27) Scragg, J. J.; Dale, P. J.; Colombara, D.; Peter, L. M. Thermodynamic Aspects of the Synthesis of Thin-Film Materials for Solar Cells. *ChemPhysChem* **2012**, *13*, 3035–3046.
- (28) Ji, S.; Shi, T.; Qiu, X.; Zhang, J.; Xu, G.; Chen, C.; Jiang, Z.; Ye, C. A Route to Phase Controllable  $\text{Cu}_2\text{ZnSn}(\text{S}_{1-x}\text{Se}_x)_4$  Nanocrystals with Tunable Energy Bands. *Sci. Rep.* **2013**, *3*, 2733.
- (29) Scragg, J.; Kubart, T.; Wätjen, J. Effects of Back Contact Instability on  $\text{Cu}_2\text{ZnSnS}_4$  Devices and Processes. *Chem. Mater.* **2013**, *25*, 3162.
- (30) Todorov, T. K.; Reuter, K. B.; Mitzi, D. B. High-Efficiency Solar Cell with Earth-Abundant Liquid-Processed Absorber. *Adv. Mater.* **2010**, *22*, E156–9.
- (31) Tsega, M.; Kuo, D.-H. The Performance of the Donor and Acceptor Doping in the Cu-Rich  $\text{Cu}_2\text{ZnSnSe}_4$  Bulks with Different Zn/Sn Ratios. *Solid State Commun.* **2013**, *164*, 42–46.
- (32) Wu, H.; Yang, R.; Song, B.; Han, Q.; Li, J.; Zhang, Y.; Fang, Y.; Tenne, R. Biocompatible Inorganic Fullerene-Nanoparticles Produced by Pulsed Laser Ablation in Water. *ACS Nano* **2011**, *5*, 1276–1281.
- (33) Grabinski, C.; Hussain, S.; Lafdi, K.; Braydich-Stolle, L.; Schlager, J. Effect of Particle Dimension on Biocompatibility of Carbon Nanomaterials. *Carbon* **2007**, *45*, 2828–2835.
- (34) Dun, C.; Holzwarth, N. A. W.; Li, Y.; Huang, W.; Carroll, D. L.  $\text{Cu}_2\text{ZnSnSxO}_{4-x}$  and  $\text{Cu}_2\text{ZnSnSxSe}_{4-x}$ : First Principles Simulations of Optimal Alloy Configurations and Their Energies. *J. Appl. Phys.* **2014**, *115*, 193513.
- (35) Gürel, T.; Sevik, C.; Çağın, T. Characterization of Vibrational and Mechanical Properties of Quaternary Compounds  $\text{Cu}_2\text{ZnSnS}_4$  and  $\text{Cu}_2\text{ZnSnSe}_4$  in Kesterite and Stannite Structures. *Phys. Rev. B* **2011**, *84*, 205201.
- (36) Mortazavi Amiri, N. B.; Postnikov, A. Electronic Structure and Lattice Dynamics in Kesterite-Type  $\text{Cu}_2\text{ZnSnSe}_4$  from First-Principles Calculations. *Phys. Rev. B* **2010**, *82*, 205204.
- (37) Search, H.; Journals, C.; Contact, A.; Iopscience, M. Theory of Space-Charge-Limited Current Enhanced by Frenkel Effect. *J. Phys. D. Appl. Phys.* **1970**, *3*, 151–156.
- (38) Persson, C. Electronic and Optical Properties of  $\text{Cu}_2\text{ZnSnS}_4$  and  $\text{Cu}_2\text{ZnSnSe}_4$ . *J. Appl. Phys.* **2010**, *107*, 053710.